

Capacity improvement of non-orthogonal multiple access downlink transmission by orbital angular momentum based mode division multiple access

Ahmed Al Amin, Soo Young Shin*

IT Convergence Engineering, Kumoh National Institute of Technology, Gumi, South Korea

Received: • Accepted/Published Online: • Final Version:

Abstract:

In this paper, non-orthogonal multiple access (NOMA) downlink transmission is integrated with orbital angular momentum (OAM) based mode division multiple access (MDMA), called NOMA-OAM-MDMA. Different OAM modes can generate different OAM waves for different superimposed signals. So, every OAM wave will be transmitted a superimposed signal from the base station to the cell center user (CCU) and cell edge user (CEU). In this way, multiple OAM waves with multiple superimposed signals will transmit from BS to CCU and CEU simultaneously to enhance the capacity of NOMA downlink transmission. Finally, the effectiveness of the proposed schemes over the existing scheme and conventional orthogonal multiple access based scheme are demonstrated through the result analysis.

Key words: Non-orthogonal multiple access, sum capacity, orbital angular momentum cell center user and cell edge user.

1. Introduction

To cope with the large channel capacity requirements of future wireless networks, non-orthogonal multiple access (NOMA) has received significant attention from the research community [1-2]. NOMA is an interesting and emerging multiple access technique that is key player for the upcoming future wireless communication network because of its main fold spectral gains [3-4]. In a power domain NOMA (PD-NOMA) based system, multiple signals are superimposed in power domain at transmitter side, by utilizing the same code at the same frequency, which is not similar than existing orthogonal multiple access (OMA) schemes such as time division multiple access (TDMA), frequency division multiple access (FDMA) and code division multiple access (CDMA). At the receiver end, signal decoding techniques such as successive interference cancellation can be performed to decode each signal. Most of the recent research is mainly focus on the channel capacity improvement in the downlink (DL) transmission of NOMA [5-6]. Which inspires the research of this paper. Previous works proposed the use of user pairing [7], the combination of OMA and NOMA [8], integration of generalized space shift keying (GSSK) with NOMA [9], and the use of coordinated multiple points (CoMP) and NOMA [10]. All of these previous works are performed to improve the capacity of DL transmission of NOMA. There is a huge potential to utilize orbital angular momentum (OAM) signals to improve the channel capacities of the DL transmission of NOMA. OAM utilizes a new degree of freedom which is known as OAM mode for signal transmission [11-12]. OAM exploits the phase variation with respect to the azimuth angle of the propagated electromagnetic waves. This leads to the helical phase structure of the wave. A system model in [13] mode division multiple access using

*Correspondence: wdragon@kumoh.ac.kr

different OAM modes (OAM-MDMA) scheme exploits different OAM modes to boost the spectral efficiency. To improve the capacities of DL NOMA, a suitable technique is required which can improve the capacities of the DL transmission to the users as well as sum capacities (SC) to a great extent without any ICI.

In this paper, NOMA is integrated with OAM-MDMA. The name of the proposed NOMA with the OAM-MDMA scheme is NOMA-OAM-MDMA in this paper. Moreover, multiple waves are created by different OAM modes. The waves are exploiting to convey additional information to the cell center user (CCU) and cell edge user (CEU) of NOMA without ICI. In addition, by utilizing the active OAM modes to transport additional information to enhance the user capacities and sum capacities as well without any additional resources (e.g. time, frequency or power). Principle contributions of this paper are briefly described as follows:

- NOMA is integrated with OAM-MDMA to improve the user capacities and SC as well.
- The capacities of CCU, CEU, and SC of the proposed NOMA-OAM-MDMA are analyzed and compared with conventional NOMA, and OMA-OAM-MDMA.
- The capacity improvement of the proposed scheme over existing schemes (e.g. NOMA) and OMA is manifested. As a benchmark, the user capacities and SC of OMA with OAM-MDMA (OMA-OAM-MDMA) are also compared with the capacities of the proposed scheme.
- The impact of normalized transmission distance between BS to CCU and number of OAM modes for NOMA-OAM-MDMA over user capacities and SC improvements of the proposed (NOMA-OAM-MDMA) scheme are analyzed and compared with conventional NOMA, and OMA-OAM-MDMA are also analyzed as well.
- By extensive computer simulations, the result analysis illustrates that the superiority of the proposed scheme over conventional NOMA, and OMA-OAM-MDMA schemes as well.

The rest of this paper is organized as follows. Section II describes the related works. Section III describes the system model and the proposed scheme explicitly. Section IV exhibits numerical result analysis. This paper is concluded in Section V.

2. Related Works

Different recent research has been done to improve the spectral efficiency of NOMA users and SC. Spatial modulation (SM) with NOMA provides improvement of channel capacities in [14]. cooperative relaying strategy is a feasible strategy to enhance the SC of the NOMA DL transmission [15-16]. Efficient resource management is another strategy to enhance the sum capacity of NOMA [17]. Moreover, a suitable solution is required to improve the channel capacities of the users and SC of NOMA DL transmission without ICI as well. So an OAM based solution can overcome the challenges of NOMA DL transmission.

OAM is a relatively new wireless communication paradigm that is attracting more and more attention for the potential short-distance line of sight (LOS) applications. Such as high-bandwidth backhaul communication for cellular networks [18]. Besides from conventional radio frequency-based communication, OAM has been extensively explored form free-space optical and fiber optic based communication system [19-20]. Moreover, mode combination in an ideal wireless OAM with Multiple Input Multiple Output (OAM-MIMO) multiplexing system can enhance the capacity of the system [21]. Which can provides better results instead of LOS-MIMO for cellular backhaul communication networks. Furthermore, [22] shows that OAM with spatial modulation provides higher capacity improvement than MIMO in case of millimeter wave communication.

3. System Model

A NOMA-OAM-MDMA network with a base station (BS) and two users (a cell-center user (CCU) and a cell-edge user (CEU)) is considered. The BS directly communicates with the CCU called as UE_1 and CEU called as UE_2 simultaneously by utilizing different signals between BS and respected users. In this case (NOMA-OAM-MDMA), total N number of OAM modes can be generated. The signals are created by utilizing a set of activated OAM modes L , where $L = \{0, 1, \dots, N-1\}$ is the set of activated OAM modes for the classical OAM-MDMA [13]. The same wave by utilizing the same OAM mode l is conveying information from BS to UE_1 and UE_2 simultaneously, where $l \in L$. The proposed network model is illustrated in Figure 1. The different waves by different OAM modes transmit a different superimposed signal to the UE_1 and UE_2 . Moreover, Two aligned uniform circular arrays (UCA) facing each other and consisting of N elements for the transmission and reception between the BS and the users [23]. Hereafter, subscript s,1, and 2 denote BS, UE_1 , and UE_2 , respectively. The distance between BS to UE_1 is $d_{s,1}$ and the distance between BS to UE_2 is $d_{s,2}$. the radii of the transmit and receive UCAs are given by r_{tx_i} and r_{rx_j} respectively [23]. The channel coefficient $h_{i,j}$ is the free space channel coefficient between any two nodes due to line-of-sight (LOS) communication [23]. Whereas, $(i, j \in \{s, UE_1, \text{and } UE_2\})$. The LOS channel with additive white gaussian noise (AWGN) is considered for all cases in this paper because OAM is performed only for LOS communication cases [13,21,23]. The data communication policy along with the signal-to-interference-plus-noise ratio (SINR) model of the proposed scheme is discussed in detail in section 3.1.

3.1. NOMA-OAM-MDMA

Following the principle of NOMA, a superimposed signal composite signal $A_l = \sqrt{p_{1l}P_l}x_{1l} + \sqrt{p_{2l}P_l}x_{2l}$ for l mode of OAM wave, where x_{1l} , x_{2l} , and p_{1l} , p_{2l} are the data symbols and the power allocation factors, respectively. Note that x_{1l} , p_{1l} and x_{2l} , p_{2l} are assigned to UE_1 and UE_2 , respectively [13,23]. In case of NOMA, $p_{1l} + p_{2l} = P_l$ and $p_{1l} < p_{2l}$. Whereas, $P = \sum_{l=0}^{N-1} P_l^2$ is the total transmit power for downlink transmission. T is the total duration of downlink transmission. Moreover, the total power allocation factor P_l for each OAM mode l from BS to the users are given below,

$$P_l = \sqrt{\frac{\frac{P}{|\xi_l|^2}}{\frac{1}{|\xi_0|^2} + \frac{1}{|\xi_l|^2} + \dots + \frac{1}{|\xi_{N-1}|^2}}}, \quad (1)$$

To radiate an OAM wave with mode number l , the same input signal A_l should be applied to the antenna element in UCA with a successive phase shift from element to the element of BS. Hence, the signal applied to the n^{th} element of BS [13, 23], where the eigenvalues of the free space LOS channels are $\xi_0, \xi_1, \dots, \xi_{N-1}$. Consequently, the superimposed signal applied to the n^{th} element in case of is given for $n = 0, \dots, N-1$ as

$$s_n^l = \frac{1}{\sqrt{N}}(A_l)e^{(-j2\pi(nl)/N)}, \quad (2)$$

With MDMA concept of OAM, the antenna element of BS $n \in \{0, 1, \dots, N-1\}$ is fed by the linear

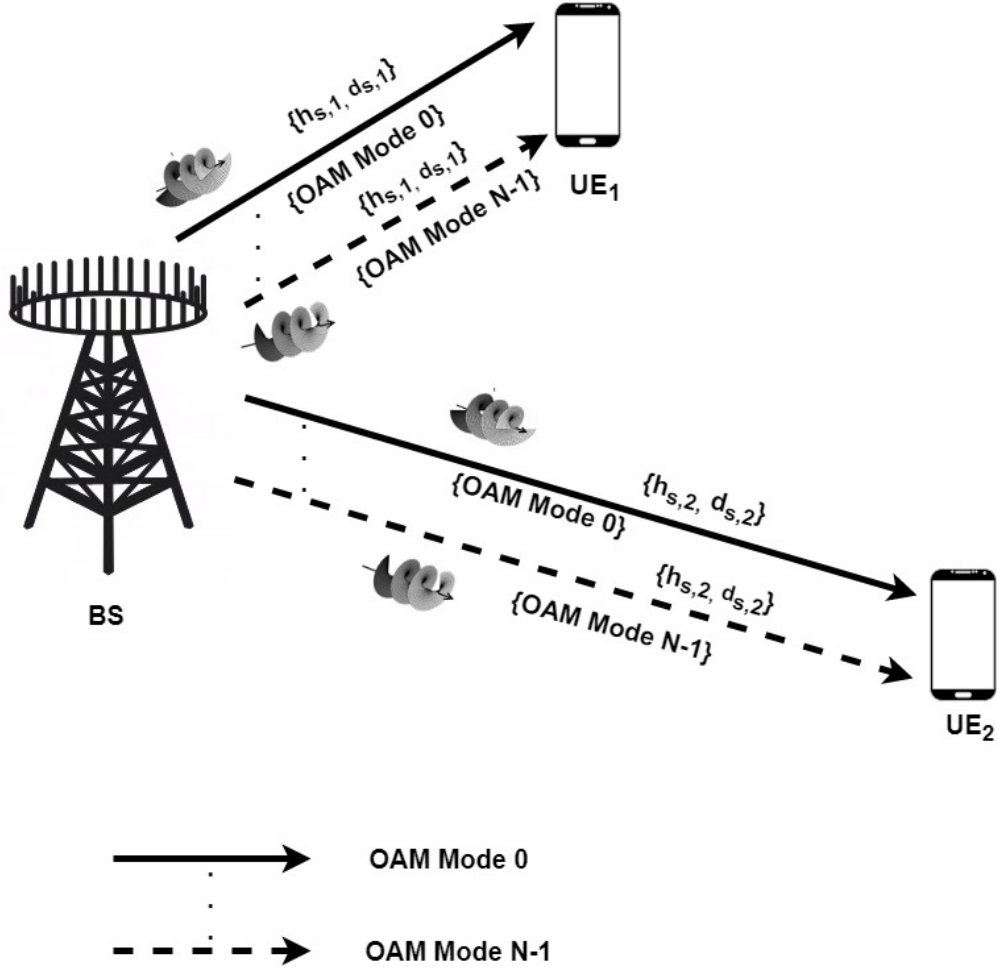


Figure 1. Proposed system model for NOMA-OAM-MDMA

superposition of the signals of different modes as [23],

$$s^n = \frac{1}{\sqrt{N}} \sum_{l \in L} (A_l) e^{(-j2\pi(nl)/N)}, \quad (3)$$

where $n = 0, 1, \dots, N-1$. For LOS propagation environment and AWGN for UE_1 and UE_2 , the free space channel response between BS to UE_1 and UE_2 are as below for OAM mode l [13,23],

$$h_{i,jl} = \beta \frac{\lambda}{4\pi d_{i,j}} e^{jkd_{n_i,p_j}}, \quad (4)$$

where, $k = \frac{2\pi}{\lambda}$, λ is the wavelength, β is a constant related with antenna gains, and in case of perfect alignment between BS and users UCAs $d_{n_i,p_j} = \sqrt{d_{i,j}^2 + r_{tx_i}^2 + r_{rx_j}^2 - 2r_{tx}r_{rx}\phi_{n_i,p_j}}$. Moreover, $\phi_{n_i,p_j} = \frac{2\pi(n_i-p_j)}{N}$ and it should be noted that due to the employment of UCAs at both BS and user sides as well as the construction of a configuration with perfect symmetry [23]. Moreover, $n_1 \sim CN(0, \sigma^2)$ and $n_2 \sim CN(0, \sigma^2)$ are

the complex AWGN at UE_1 and UE_2 respectively with zero mean and variance σ^2 . Moreover, $|h_{s,1}|^2 > |h_{s,2}|^2$ because $d_{s,1} < d_{s,2}$ is considered in this paper. The demultiplexed and recovered receive signal at UE_1 and UE_2 are respectively given by [13,23]

$$y_{1l} = \frac{1}{\sqrt{N}} \sum_{p_1=0}^{N-1} (y_{1p_1}) e^{(-j2\pi(p_1l)/N)} + n_1, \quad (5)$$

$$y_{2l} = \frac{1}{\sqrt{N}} \sum_{p_2=0}^{N-1} (y_{2p_2}) e^{(-j2\pi(p_2l)/N)} + n_2, \quad (6)$$

for $l = 0, 1, \dots, N-1$, where y_{1l} and y_{2l} are the p_1 th or p_2 th element of received signal by UE_1 and UE_2 respectively. According to the downlink NOMA protocol, UE_1 first decodes x_2 and then performs SIC to decode own symbol x_1 . Thus, the received SINR at UE_1 in case of x_1 and x_2 are respectively given by following equations due to received OAM wave with l mode,

$$\gamma_{x_{1l}}^{UE_1} = \rho_l |h_{s,1l}|^2 p_1, \quad (7)$$

$$\gamma_{x_{2l}}^{UE_1} = \frac{\rho_l |h_{s,1l}|^2 p_2}{\rho_l |h_{s,1l}|^2 p_1 + 1}, \quad (8)$$

where $\rho_l \triangleq \frac{P_l}{\sigma^2}$ is the transmit signal-to-noise ratio (SNR) by BS for OAM mode l and total transmit SNR, $\rho = \sum_{l=0}^{N-1} \rho_l$. The signal can be directly decoded at UE_2 by treating the signal x_1 as noise. Therefore, the received SINR at UE_2 in case of x_2 is given by following equations due to received OAM wave with l mode,

$$\gamma_{x_{2l}}^{UE_2} = \frac{\rho_l |h_{s,2l}|^2 p_2}{\rho_l |h_{s,2l}|^2 p_1 + 1}, \quad (9)$$

3.2. Achievable capacity analysis

By considering normalized total time duration $T = 1$ for downlink transmission. The equations for the capacities are derived in the following segments.

3.2.1. Capacity of UE_1

x_{1l} and x_{2l} are received by UE_1 for OAM mode l . So, the achievable capacity of UE_1 for the wave with OAM mode l is obtained as below by Eq. 6,

$$C_{UE_{1l}} = \log_2(1 + \mu_{1,l} \gamma_{x_{1l}}^{UE_1}), \quad (10)$$

Where, $\mu_{1,l}$ is the singular value of the channel response matrix $h_{s,1l}$ for OAM mode l . So, the total channel capacity at UE_1 for all the OAM wave from BS to UE_1 is as below,

$$C_{UE_1} = \sum_{l=0}^{N-1} \log_2(1 + \mu_{1,l} \gamma_{x_{1l}}^{UE_1}), \quad (11)$$

3.2.2. Capacity of UE_2

x_{2_l} is directly decoded by UE_2 by treating x_{1_l} as noise. So, the achievable capacity of UE_2 for the wave with OAM mode l is obtained as below by Eq. 8,

$$C_{UE_{2l}} = \log_2(1 + \mu_{2,l}\gamma_{x_{2_l}}^{UE_2}), \quad (12)$$

Where, $\mu_{2,l}$ is the singular value of the channel response matrix $h_{s,2l}$ for OAM mode l . So, the total channel capacity at UE_2 for all the OAM wave from BS to UE_2 is as below,

$$C_{UE_2} = \sum_{l=0}^{N-1} \log_2(1 + \mu_{2,l}\gamma_{x_{2_l}}^{UE_2}), \quad (13)$$

3.2.3. Sum Capacity

So, the SC can be achieved by adding Eq. 11 and Eq. 13 as below,

$$C_{SC} = C_{UE_1} + C_{UE_2} \quad (14)$$

3.3. OMA-OAM-MDMA

For a fair comparison with the proposed NOMA-OAM-MDMA scheme, the OMA-OAM-MDMA scheme is also devised in this paper as a benchmark, taking into account time-division multiple access. It should be mentioned that eight time slots are required for completing data transmission in OMA-OAM-MDMA, whereas only one time slot is required in the proposed NOMA-OAM-MDMA scheme. The capacities of the users and the SC are given by

$$C_{UE_1}^{OMA} = \frac{1}{8} \sum_{l=0}^{N-1} \log_2(1 + \mu_{1,l}\rho_l|h_{s,1l}|^2). \quad (15)$$

$$C_{UE_2}^{OMA} = \frac{1}{8} \sum_{l=0}^{N-1} \log_2(1 + \mu_{2,l}\rho_l|h_{s,2l}|^2). \quad (16)$$

So, the SC can be achieved by adding Eq. 15 and Eq. 16 as below,

$$C_{SC}^{OMA} = C_{UE_1}^{OMA} + C_{UE_2}^{OMA}. \quad (17)$$

3.4. Numerical Results

In this section computer simulation results for the user capacities and SC of the proposed scheme are examined as well as explained. The impact of changes in transmit SNR ρ , normalized transmission distance between BS and CCU $\tilde{d}_{s,1}$ are discussed. Collinear placement of all nodes (e.g. BS, UE_1 , and UE_2 and normalized distances between any two nodes are considered, where $d_{s,1} = 500\lambda$, $d_{s,2} = 1000\lambda$. The wave length $\lambda = 0.03$, $T = 1$, $L = \{0, 1, 2, 3\}$ (For 4 modes of OAM), $L = \{0, 1\}$ (For 2 modes of OAM) and $P = 1$ are considered as well for simulation purpose. For performance comparison, simulation results for CCU capacity (UE_1 capacity), CEU capacity (UE_2 capacity) and SC of NOMA-OAM-MDMA, conventional NOMA and OMA-OAM-MDMA are also provided. In the ideal case, each receiver is located in the OAM circle region of OAM signals with

required OAM mode by utilizing the directional characteristics of OAM beam. Note that, similar simulation parameters are considered for the proposed and compared schemes for consistency.

Impact of ρ , $d_{s,1}$ and N on CCU capacity, CEU capacity and SC of the proposed system is shown in this part. All figures are plotted for different LOS channels from BS to CCU and CEU for different OAM signals.

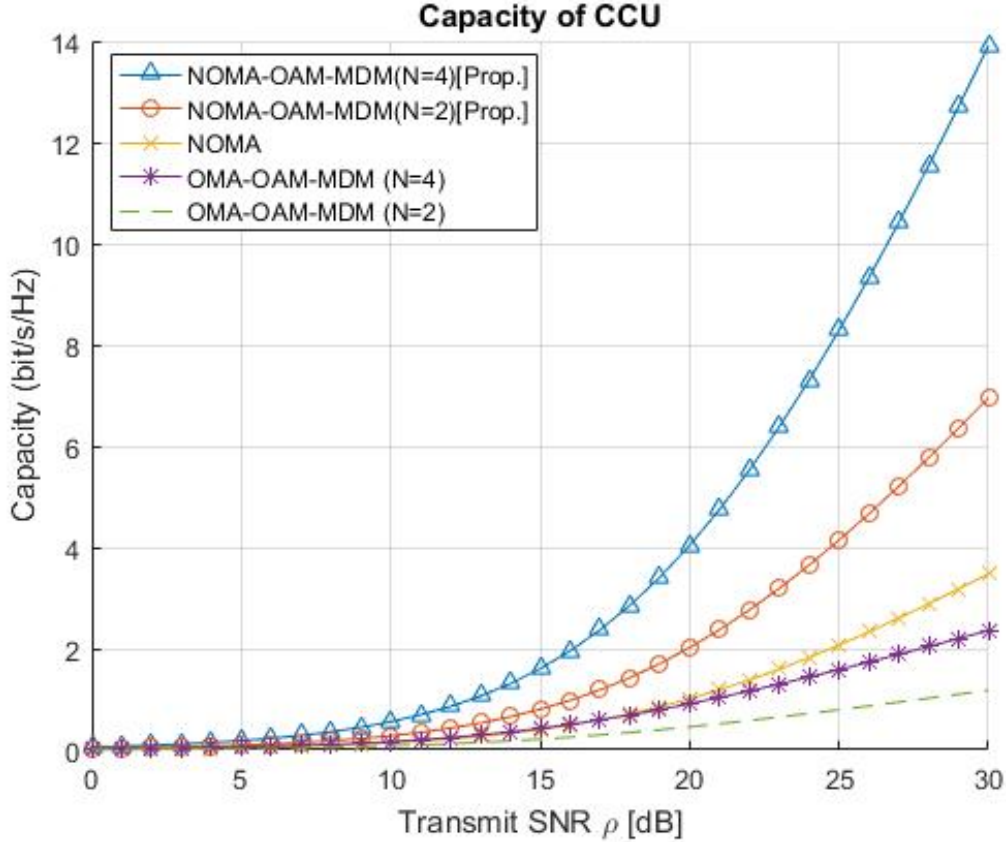


Figure 2. Capacity comparisons of CCU with respect to transmit SNR $p_1 = 0.4$, $p_2 = 0.6$, $P = 1$, $T = 1$, $\lambda = 0.03$, $d_{s,1} = 500\lambda$, and $d_{s,2} = 1000\lambda$.

The capacity of CCU (UE_1) with respect to (w.r.t.) transmit SNR ρ is demonstrated in Figure 2 for the proposed NOMA-OAM-MDMA ($N = 4$ and $N = 2$) and compared with existing NOMA, and OMA-OAM-MDMA ($N = 4$ and $N = 2$). Parameters $p_1 = 0.4$, and $p_2 = 0.6$ are set during the simulation. The CCU capacity of all schemes increases linearly with an increase of ρ . The proposed scheme (NOMA-OAM-MDMA) exhibits far better performance than conventional NOMA and other OMA-OAM-MDMA schemes. Moreover, larger set of OAM modes $L = \{0, 1, 2, 3\}$ due to $N = 4$ for the proposed scheme provides much better capacity for CCU than lower set of OAM signals $L = \{0, 1\}$ due to $N = 2$. Because of the higher number of OAM signals carrying much more superimposed signals than a lower number of signals without ICI. This is performed by utilizing OAM based MDMA for different OAM signals. The OAM signals are generated by each different OAM modes. As a result, the capacity of CCU is enhanced significantly compared to other schemes. The same phenomena happened to the OMA-OAM-MDMA case as well. A higher number of signals provides much better capacity than the lower number of OAM signals. Moreover, due to utilizing separate time slot for each

transmission the CCU capacity of OMA-OAM-MDMA schemes are far lower than the proposed scheme with the higher number of OAM signals which is illustrated in Figure 2 as well.

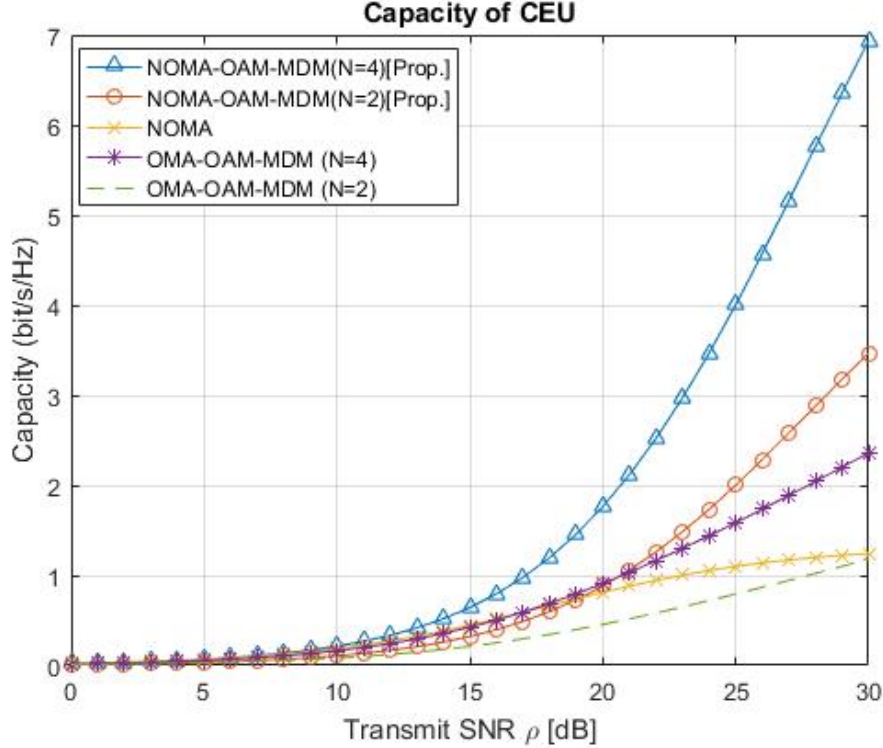


Figure 3. Capacity comparisons of CEU with respect to transmit SNR $p_1 = 0.4$, $p_2 = 0.6$, $P = 1$, $T = 1$, $\lambda = 0.03$, $d_{s,1} = 500\lambda$, and $d_{s,2} = 1000\lambda$.

The capacity of CEU (UE_2) with respect to (w.r.t.) transmit SNR ρ is demonstrated in Figure 3 for the proposed NOMA-OAM-MDMA ($N = 4$ and $N = 2$) and compared with existing NOMA, and OMA-OAM-MDMA ($N = 4$ and $N = 2$). Parameters $p_1 = 0.4$, and $p_2 = 0.6$ are set during the simulation. The CEU capacity of all schemes increases linearly with an increase of ρ . The proposed scheme (NOMA-OAM-MDMA) exhibits far better performance than conventional NOMA and other OMA-OAM-MDMA schemes. Moreover, higher set of OAM modes $L = \{0, 1, 2, 3\}$ due to $N = 4$ for the proposed scheme provides much better capacity for CEU than lower set of OAM modes $L = \{0, 1\}$ due to ($N = 2$). Because of the higher number of signals carrying much more superimposed signals than a lower number of signals without ICI like as CCU. This is performed by utilizing OAM based MDMA for different OAM signals. The OAM signals are generated by each different OAM modes. As a result, the capacity of CEU is enhanced significantly compared to other schemes. The same phenomena happened to the OMA-OAM-MDMA case as well. A higher number of signals provides much better capacity than the lower number of OAM signals. Moreover, due to utilizing separate time slot for each transmission the CEU capacity of OMA-OAM-MDMA schemes are far lower than the proposed scheme with the higher number of OAM signals which is illustrated also in Figure 3.

In Figure 4, proposed NOMA-OAM-MDMA provides significantly higher SC than other compared schemes. Parameters $p_1 = 0.4$, and $p_2 = 0.6$ are set during the simulation. Moreover, higher N provides better SC than lower N for the proposed scheme as well. These phenomena happen because the CCU and CEU

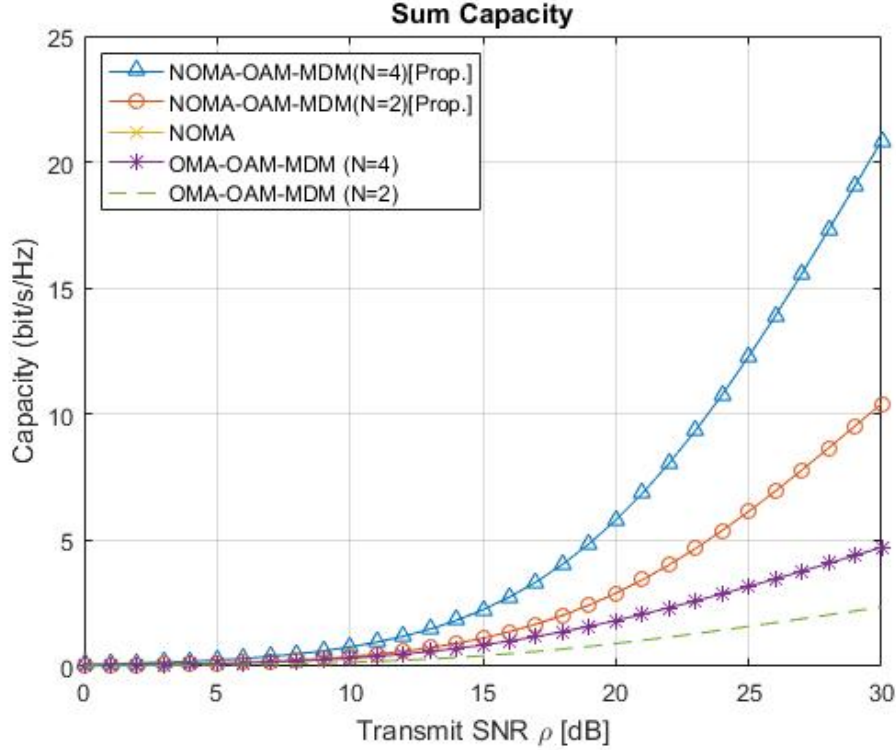


Figure 4. SC with respect to transmit SNR $p_1 = 0.4$, $p_2 = 0.6$, $P = 1$, $T = 1$, $\lambda = 0.03$, $d_{s,1} = 500\lambda$, and $d_{s,2} = 1000\lambda$.

capacity is higher for the proposed scheme. Moreover, the higher number of L due to the higher number of N carrying much more superimposed signals to the CCU and CEU by utilizing OAM-MDMA for different modes of OAM as well. Hence, the proposed NOMA-OAM-MDMA scheme with a higher $N = 4$ provides significantly higher SC than other compared schemes as well.

The impact of normalized transmission distance between BS to CCU $\tilde{d}_{s,1}$ on CCU capacity is illustrates in Figure 5, where $\tilde{d}_{s,1} = \frac{d_{s,1}}{d_{s,2}}$. Parameters $p_1 = 0.4$, $p_2 = 0.6$, and $\rho = 25dB$ are set during the simulation. The CCU capacity is decreasing for increasing values of $\tilde{d}_{s,1}$. The proposed scheme NOMA-OAM-MDMA provides better capacity for CCU due to variation of $\tilde{d}_{s,1}$. Moreover, higher values of N for the proposed scheme provides significantly higher CCU channel capacity than other compared scheme. This enhancement is achieve at CCU because higher number of signals (For $N = 4$ provides $L = \{0, 1, 2, 3\}$ and For $N = 2$ provides $L = \{0, 1\}$) conveying higher number of superimposed signals to the CCU. So the CCU capacity is enhanced for the proposed scheme with higher number of N for the proposed scheme.

The impact of normalized transmission distance between BS to CCU $\tilde{d}_{s,1}$ on CEU capacity is illustrates in Figure 6. Parameters $p_1 = 0.4$, $p_2 = 0.6$, and $\rho = 25dB$ are set during the simulation. In this analysis the position of CCU is varying but the position of CEU is remain steady. Hence the CEU capacity is steady for increasing values of $\tilde{d}_{s,1}$. Because the transmission distance between BS and CEU $d_{s,2}$ and ρ are remain constant in this case. Moreover, the proposed scheme with higher N outplayed other compared schemes in this observation as well. This enhancement is achieve at CEU because higher number of signals (For $N = 4$ provides

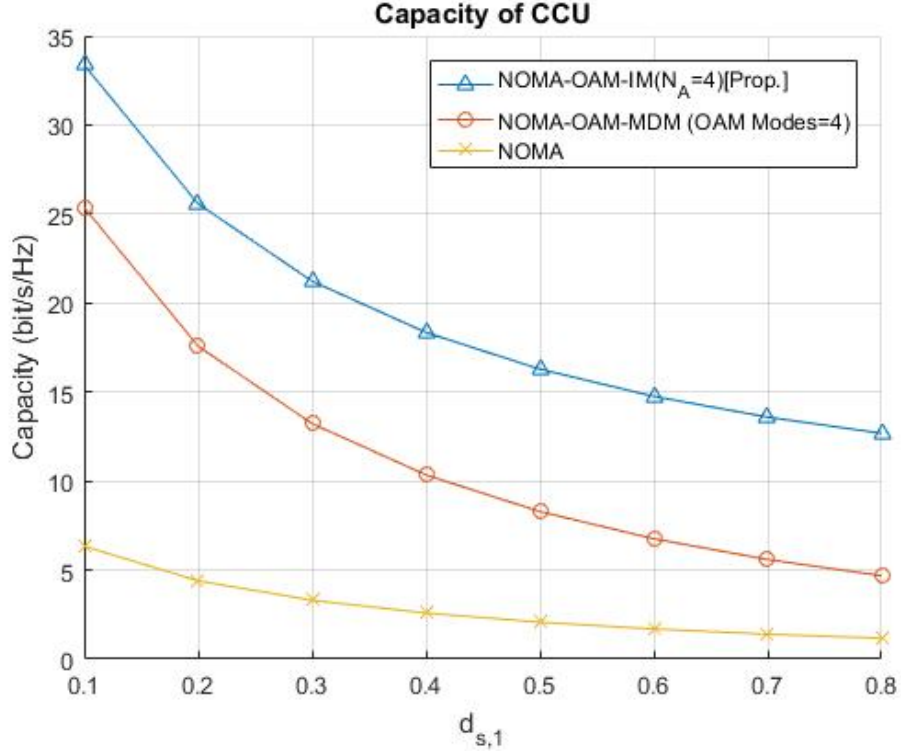


Figure 5. CCU Capacity with respect to $d_{s,1}$ $p_1 = 0.4$, $p_2 = 0.6$, $P = 1$, $T = 1$, $\lambda = 0.03$, $\rho = 25dB$

$L = \{0, 1, 2, 3\}$ and For $N = 2$ provides $L = \{0, 1\}$) conveying higher number of superimposed signals to the CEU. So, the CEU capacity is enhanced for the proposed scheme with higher number of N for the proposed NOMA-OAM-MDMA scheme.

The impact of normalized transmission distance between BS to CCU $\tilde{d}_{s,1}$ on SC is illustrates in Figure 7. Parameters $p_1 = 0.4$, $p_F = 0.6$, and $\rho = 25dB$ are set during the simulation. The SC is decreasing for increasing values of $\tilde{d}_{s,1}$ because the CCU capacity is decreasing for increasing values of $\tilde{d}_{s,1}$. This phenomena is shown in Figure 5. Moreover, the CEU capacity is steady for the proposed scheme and others as well. In addition, the proposed NOMA-OAM-MDMA scheme provides significantly SC than other compared schemes for higher N . Because higher values of N provides higher CCU and CEU capacities which is shown in Figure 5 and Figure 6. As a matter of fact the SC is also improved as well for the proposed scheme with higher N compared to NOMA-OAM-MDMA ($N = 2$), conventional NOMA, OMA-OAM-MDMA ($N = 4$), and OMA-OAM-MDMA ($N = 2$).

4. Conclusion

In this paper, the NOMA-OAM-MDMA scheme has been proposed to enhance the user capacities and SC of NOMA downlink transmission. Moreover, conventional NOMA and OMA-OAM-MDMA are also compared with the proposed scheme for a fair comparison. According to result analysis, it is shown that the proposed scheme with the higher number of OAM signals provides improved performance compared to other conventional schemes in terms of capacities. In the future, the work can be extended by incorporating relay assisted CNOMA

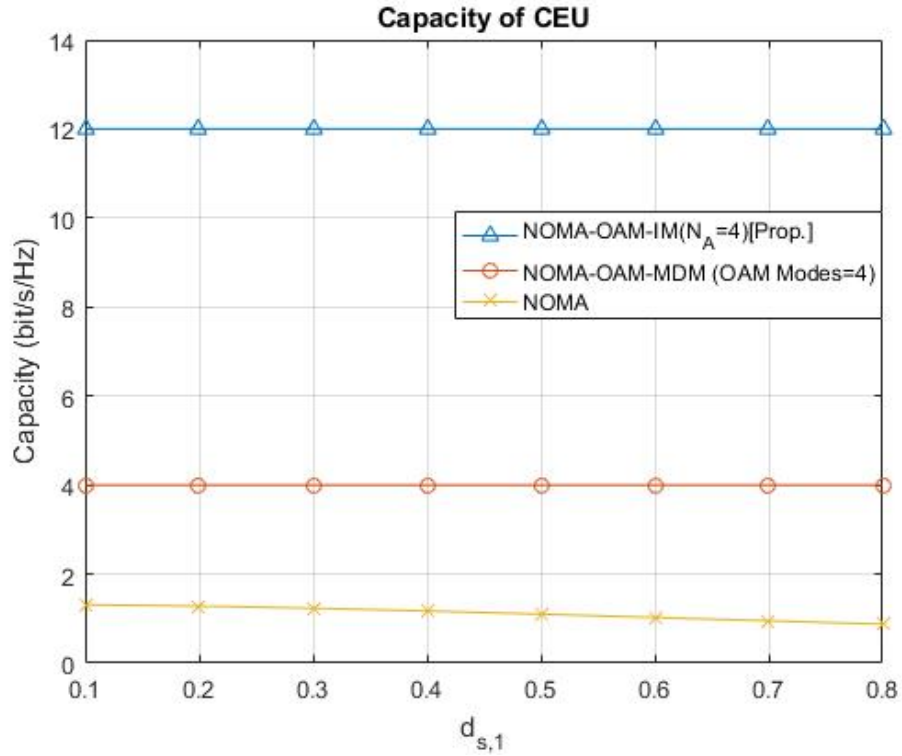


Figure 6. CEU Capacity with respect to $d_{s,1}$ $p_1 = 0.4$, $p_2 = 0.6$, $P = 1$, $T = 1$, $\lambda = 0.03$, $\rho = 25dB$

with the proposed scheme.

Acknowledgment

This work was supported by the National Research Foundation of Korea(NRF) grant funded by the Korea government(MEST) (No. 2019R1A2C1089542)

References

- [1] Kader, M. F., Shahab, M. B., and Shin, S. Y., Non-orthogonal multiple access for a full-duplex cooperative network with virtually paired users. *Computer Communications*, 2018; 120: 1–9.
- [2] Higuchi, K., and Benjebbour, A., Non-orthogonal Multiple Access (NOMA) with Successive Interference Cancellation for Future Radio Access. *IEICE Transactions on Communications*, 2015; E98: 403–414.
- [3] Basharat M, Ejaz W, Naeem M, Khattak AM, Anpalagan A. A survey and taxonomy on nonorthogonal multiple-access schemes for 5G networks. *Trans Emerging Tel Tech*. 2018, 29:1-17.
- [4] Dai L, Wang B, Yuan Y, Han S, Chih-Lin I, Wang Z. Non-orthogonal multiple access for 5G: solutions, challenges, opportunities, and future research trends. *IEEE Commun Mag*. 2015; 53:74-81.
- [5] Kimy, B., Lim, S., Kim, H., Suh, S., Kwun, J., Choi, S., Hong, D. . Non-orthogonal Multiple Access in a Downlink Multiuser Beamforming System. *MILCOM 2013 - 2013 IEEE Military Communications Conference*, 2013.
- [6] Ali, M. S., Hossain, E., and Kim, D. I., Non-Orthogonal Multiple Access (NOMA) for Downlink Multiuser MIMO Systems: User Clustering, Beamforming, and Power Allocation. *IEEE Access*, 2017; 5:565–577.

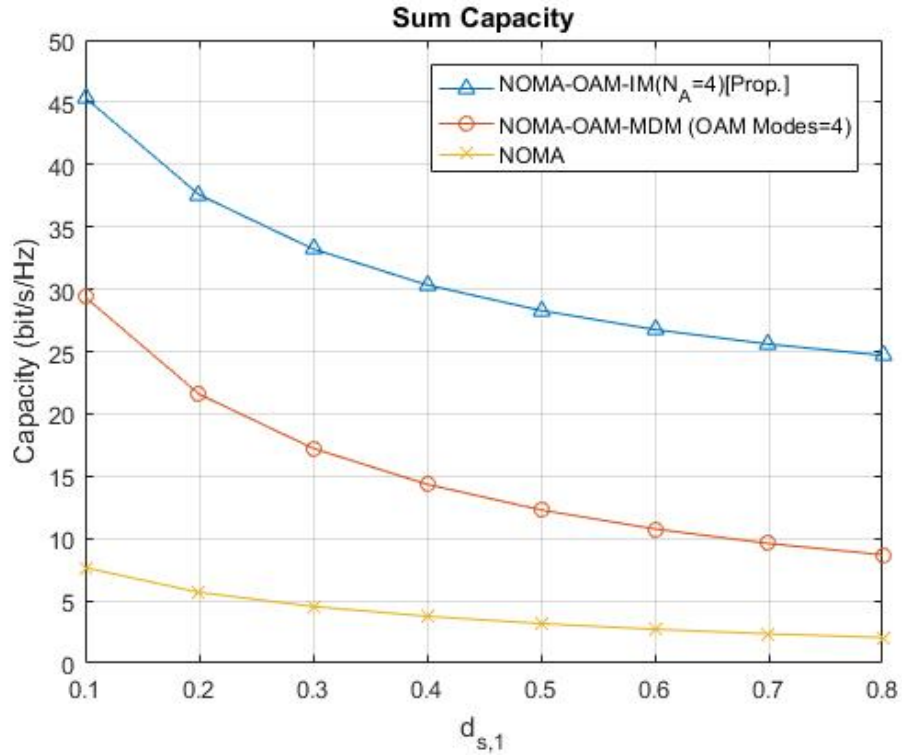


Figure 7. SC with respect to $d_{s,1}$ $p_1 = 0.4$, $p_2 = 0.6$, $P = 1$, $T = 1$, $\lambda = 0.03$, $\rho = 25dB$

- [7] Shahab, M. B., Kader, M. F., and Shin, S. Y., A Virtual User Pairing Scheme to Optimally Utilize the Spectrum of Unpaired Users in Non-orthogonal Multiple Access. *IEEE Signal Processing Letters*, 2016; 23: 1766–1770.
- [8] Janghel, K., and Prakriya, S. Performance of Adaptive OMA/Cooperative-NOMA Scheme With User Selection. *IEEE Communications Letters*, 2018; 22: 2092–2095.
- [9] Kim, J. W., Shin, S. Y., and Leung, V. C. M., Performance Enhancement of Downlink NOMA by Combination With GSSK. *IEEE Wireless Communications Letters*, 2018; 7: 860–863.
- [10] Tian, Y., Nix, A. R., and Beach, M., On the Performance of Opportunistic NOMA in Downlink CoMP Networks. *IEEE Communications Letters*, 2016; 20: 998–1001.
- [11] Jiang, X., Zhao, Y., and Zhang, C., Capacity evaluation on the long-distance orbital angular momentum non-orthogonal transmission. 2018 IEEE MTT-S International Wireless Symposium (IWS), 2018.
- [12] Wang, L., Ge, X., Zi R. and Wang, C., "Capacity Analysis of Orbital Angular Momentum Wireless Channels, *IEEE Access*, 2017; 5: pp. 23069-23077.
- [13] Wang, L., Jiang, F., Yuan, Z., Yang, J., Gui, G., and Sari, H. . Mode division multiple access: a new scheme based on orbital angular momentum in millimetre wave communications for fifth generation. *IET Communications*, 2018; 12: 1416–1421.
- [14] Zhu, X., Wang, Z., and Cao, J., NOMA-Based Spatial Modulation. *IEEE Access*, 2017; 5: 3790–3800.
- [15] Duan, W., Zhang, G., Sun, Q., Hou, J., Ji, Y., and Choi, J., On the performance of an enhanced transmission scheme for cooperative relay networks with NOMA. *EURASIP Journal on Wireless Communications and Networking*, 2018; 1.
- [16] Kader, M. F., Shin, S. Y., and Leung, V. C. M., Full-Duplex Non-Orthogonal Multiple Access in Cooperative Relay Sharing for 5G Systems. *IEEE Transactions on Vehicular Technology*, 2018; 67: 5831–5840.

- [17] Ali, A., Baig, A., Awan, G. M., Khan, W. U., Ali, Z., and Sidhu, G. A. S., Efficient Resource Management for Sum Capacity Maximization in 5G NOMA Systems. *Applied System Innovation*, 2019; 2: 27.
- [18] Tamagnone, M., Craeye, C., and Perruisseau-Carrier, J. (2013). Encoding many channels on the same frequency through radio vorticity: first experimental test. *New Journal of Physics*, 2013; 15.
- [19] Willner, A. E, Communication with a twist. *IEEE Spectrum*, 2016; 53: 34–39.
- [20] Lee, D., Sasaki, H., Fukumoto, H., Hiraga, K., and Nakagawa, T, Orbital Angular Momentum (OAM) Multiplexing: An Enabler of a New Era of Wireless Communications. *IEICE Transactions on Communications*, 2017; B: 1044–1063.
- [21] Opore, K. A., Kuang, Y., and Kponyo, J. J, Mode Combination in an Ideal Wireless OAM-MIMO Multiplexing System. *IEEE Wireless Communications Letters*, 2015; 4: 449–452.
- [22] Ge, X., Zi, R., Xiong, X., Li, Q., and Wang, L., Millimeter wave communications with OAM-SM scheme for future mobile networks. *IEEE Journal on Selected Areas in Communications*, 2017; 35: 2163-2177..
- [23] Basar, E., Orbital Angular Momentum With Index Modulation. *IEEE Transactions on Wireless Communications*, 2018; 17: 2029–2037.